Pyrazolo[4,3-*e*]-1,2,4-triazolo[1,5-*c*]pyrimidine Derivatives as Adenosine Receptor Antagonists. Influence of the N5 Substituent on the Affinity at the Human A_3 and A_{2B} Adenosine Receptor Subtypes: A Molecular Modeling Investigation

Giorgia Pastorin,[†] Tatiana Da Ros,[†] Giampiero Spalluto,*[,†] Francesca Deflorian,[#] Stefano Moro,*[,#] Barbara Cacciari,[§] Pier Giovanni Baraldi,*[,§] Stefania Gessi,[‡] Katia Varani,[‡] and Pier Andrea Borea[‡]

Dipartimento di Scienze Farmaceutiche, Università degli Studi di Trieste, Piazzale Europa 1, I-34127 Trieste, Italy, Dipartimento di Scienze Farmaceutiche, Università degli Studi di Ferrara, Via Fossato di Mortara 17-19, I-44100 Ferrara, Italy, Molecular Modeling Section, Dipartimento di Scienze Farmaceutiche, Università di Padova, via Marzolo 5, I-35131 Padova, Italy, and Dipartimento di Medicina Clinica e Sperimentale-Sezione di Farmacologia, Università degli Studi di Ferrara, Via Fossato di Mortara 17-19, I-44100 Ferrara, Italy

Received March 25, 2003

A new series of pyrazolo[4,3-*e*]-1,2,4-triazolo[1,5-*c*]pyrimidines bearing various substituents at both the N5-pyrimidinyl and N8-pyrazolyl positions have been synthesized, and their binding affinities at the four human adenosine receptor subtypes (hA_1, hA_{2A}, hA_{2B}, and hA_3) have been evaluated. All the described compounds contain arylacetyl moieties at the N5 position and arylalkyl substituents at the N8 position. Surprisingly, all the compounds present their most potent affinities at the hA_{2B} adenosine receptor with a range of selectivities against the other subtypes. When bulky groups are present simultaneously at the N5 and N8 positions (e.g., compound **9**), the best selectivity for the hA_{2B} receptor was observed ($K_i(hA_1) = 1100$ nM; $K_i(hA_{2A}) = 800$ nM; $K_i(hA_{2B}) = 20$ nM; $K_i(hA_3) = 300$ nM, $K_i(hA_1/A_{2B}) = 55$, $K_i(hA_{2A}/A_{2B}) = 40$, $K_i(hA_3/hA_{2B}) = 15$). To understand the molecular significance of these results, we compared the putative TM (transmembrane) binding motif of compound **9** on both hA_{2B} and hA_3 receptors. From our docking studies, compound **9** fits neatly inside the TM region of the hA_{2B} receptor but not in the corresponding hA_3 region, illustrating significant differences between the two subtypes. The study herein presented permits an understanding of why the bioisosteric replacement of an −NH, present in previously reported hA_3 receptor antagonists, with a $-CH_2$ group at the N5 position induces such large differences in hA_{2B}/hA_3 affinity. In the molecular structure of the hA_3 receptor, two residues, Ser243 (TM6) and Ser271 (TM7), create a hydrophilic region, which seems to permit a better accommodation of the phenylurea series into this putative hA_3 binding site than the phenylacetyl series.

Introduction

It is widely reported that adenosine is a ubiquitous modulator that exerts its functions through interaction with four G-coupled receptors classified as A_1, A_{2A}, A_{2B}, and A_3.[1] While A_1 and A_{2A} receptors are stimulated by low doses of adenosine, A_{2B} and A_3 subtypes require higher concentrations of the natural ligand.[2,3] During the years, intensive efforts by medicinal chemists allowed the discovery of potent and selective ligands (agonists and antagonists) for the adenosine A_1, A_{2A}, and A_3 receptor subtypes.[4,5] For only the A_{2B} subtypes, scientists are aiming to obtain potent and selective antagonists in order to better understand the pathophysiological role of this receptor subtype.[6−8]

In the past few years, significant advancement has been made in the understanding of the molecular pharmacology and physiology of the A_{2B} adenosine receptors, but because of the lack of highly potent and selective ligands for this receptor subtype, many questions have not yet been answered.[5−7] A_{2B} receptors appear to be implicated in the regulation of mast cell secretion,[8,9] gene expression,[10] cell growth,[11] intestinal functions,[12] and vascular tone.[13] They play also a role in asthma, mediating mast cell degranulation from the rat RBL mastlike cells and being present in high density in the human blood eosinophils.[5,6,14] For these reasons, the use of A_{2B} antagonists could be proposed as antiasthmatic agents.[5,6,14]

In this field of research, some structure−activity relationship studies have been reported. However, at present only few examples of quite potent and selective hA_{2B} adenosine antagonists are available. Only recently, some xanthine congeners structurally related to XAC (8[4-[[[(2-aminoethyl)amino]carbonyl]methyloxy]phenyl]-1,3-dipropylxanthine) have been demonstrated to be potent A_{2B} antagonists by Jacobson and co-workers.[15−17] An improvement of this work has been published by Muller et al.,[18,19] which described some interesting 1,8-disubstituted xanthine derivatives with good affinity,

* To whom correspondence should be addressed. For G.S.: phone, +39-(0)40-5582525; fax, +39-(0)40-52572; e-mail, spalluto@univ.trieste.it. For S.M.: phone, +39-049-8275704; fax, +39-049-8275366; e-mail, stefano.moro@unipd.it. For P.G.B.: phone, +39-0532-291293; fax, +39-0532-291296; e-mail, pgb@unife.it.

[†] Università degli Studi di Trieste.

[#] Università di Padova.

[§] Dipartimento di Scienze Farmaceutiche, Università degli Studi di Ferrara.

[‡] Dipartimento di Medicina Clinica e Sperimentale-Sezione di Farmacologia, Università degli Studi di Ferrara.

10.1021/jm030852k CCC: $25.00
Published on Web 08/30/2003

Chart 1. Rational Design of Synthesized Compounds as hA_{2B} Adenosine Receptor Antagonists (Binding Data Taken from Refs 23 and 24)

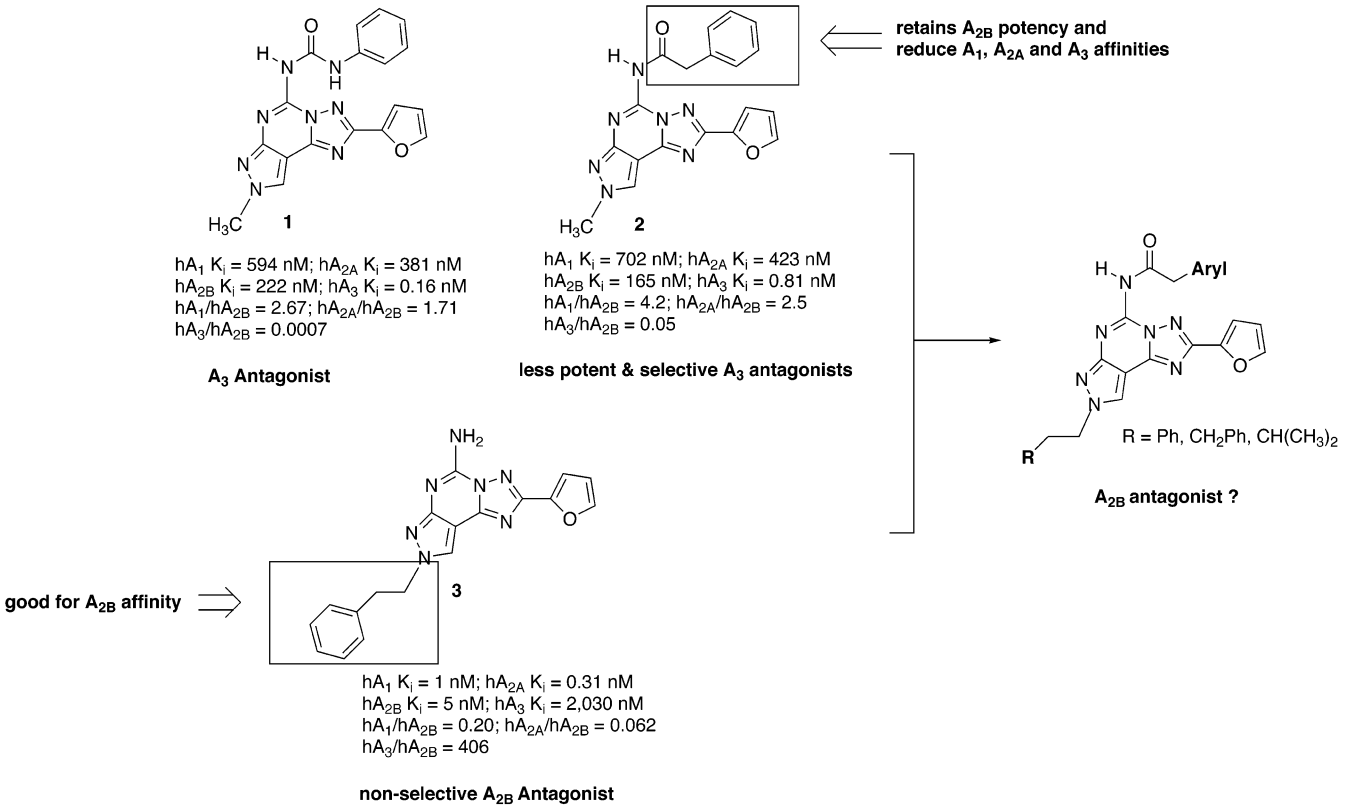

selectivity, and moreover, water solubility. In the non-xanthine family, some triazolotriazine[20] or triazoloquinazoline[21] derivatives have been reported as A_{2B} antagonists, but none of the synthesized compounds showed significant potency and/or selectivity for this receptor subtype.

Very recently, some promising quinazoline derivatives have been investigated by Jacobson and co-workes as A_{2B} adenosine receptor antagonists. In particular, a compound named CMB 6466 (4-methyl-7-methoxyquinazolyl-2-(2′-amino-4′-imidazolinone)) showed an interesting affinity ($K_i(hA_{2B}) = 112$ nM) and proved to be quite selective against rA_1 and rA_{2A} adenosine receptor subtypes.[22] In a rational screening program focused on searching new non-xanthine A_{2B} adenosine receptor antagonists, we decided to investigate a new series of pyrazolotriazolopyrimidine derivatives as A_{2B} adenosine receptor antagonists. This project was based on some previous experimental observations on different substituted pyrazolotriazolopyrimidines. In particular, we observed that the introduction at the N5 position of a phenylacetyl moiety (**2**) produces a significant decrease of affinity at the hA_3 adenosine receptors with respect to the aryl carbamoyl moiety typical of hA_3 adenosine receptor antagonists (**1**), with a simultaneous retention or a slight increase of affinity at the hA_{2B} adenosine receptor subtype[23] (Chart 1).

In a parallel study on N5-unsubstituted pyrazolotriazolopyrimidines, we observed that the presence of an aryl or a branched chain at the N8 position (**3**) is favorable for the interaction with the hA_{2B} adenosine receptors, even though no significant selectivity vs other receptor subtypes was observed.[24] For this reason, we decided to synthesize some hybrid molecules bearing an arylacetyl moiety at the N5 position and simultaneously aryl or branched chain at the N8 position. This approach has been utilized to obtain potential A_{2B} adenosine receptor antagonists and also to evaluate the effect of the substitution at the N5 position on the hA_3 and A_{2B} receptors recognition, by molecular modeling studies.

Results and Discussion

The desired compounds (**4**−**12**) were prepared by acylation with the appropriate arylacetyl chloride (1.3 equiv) of the well-known and previously reported unsubstituted derivatives **13**−**15**[25−27] in dry THF at reflux (18 h) in the presence of trietylamine (1.3 equiv) (Table 1).

In Table 1 the receptor binding affinities of the synthesized compounds (**4**−**12**) are also reported. They were determined at the human A_1, A_{2A}, A_{2B}, and A_3 receptors expressed in CHO (A_1, A_{2A}, A_3) and HEK-293 (A_{2B}) cells. [^{3}H]-1,3-dipropyl-8-cyclopentylxanthine ([^{3}H]DPCPX)[28,29] (A_1 and A_{2B}), [^{3}H]-4-[2-[[7-amino-2-(2-furyl)-1,2,4-triazolo[2,3-*a*]-1,3,5triazin-5-yl]amino]ethyl]phenol ([^{3}H]-ZM241385) (A_{2A}),[30] and [^{3}H]-5-(4-methoxyphenylcarbamoyl)amino-8-propyl-2-(2-furyl)pyrazolo[4,3-*e*]-1,2,4-triazolo[1,5-*c*]pyrimidine ([^{3}H]-MRE3008-F20) (A_3)[29] have been used as radioligands in binding assays.

All the synthesized compounds showed affinity at the A_{2B} adenosine receptor subtype in the nanomolar range (20−40 nM) with different degrees of selectivity versus the other receptor subtypes (1- to 55-fold). Remarkably, the affinity at the A_{2B} adenosine receptors is almost similar for all derivatives, independent of the nature of the substitution at both the N5 and N8 positions. In contrast, these substitutions seem to modulate significantly the affinity against the other receptor subtypes, with a consequent influence on the selectivity. In

Table 1. Structures, Synthesis, and Binding Affinities at hA_1, hA_{2A}, hA_{2B}, and hA_3 Adenosine Receptors of Synthesized Compounds

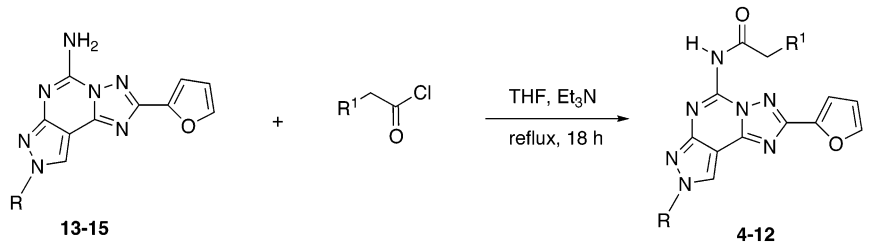

			K_i (nM)				ratio of K_i values		
compd	R	R^1	hA_1[a]	hA_{2A}[b]	hA_{2B}[c]	hA_3[d]	hA_1/hA_{2B}	hA_{2A}/hA_{2B}	hA_3/hA_{2B}
4	$(CH_3)_2CHCH_2CH_2$	Ph	200 ± 23	57 ± 4	31 ± 3	81 ± 6	6.4	1.8	2.6
5	$PhCH_2CH_2$	Ph	120 ± 14	60 ± 7	35 ± 5	45 ± 5	3.4	1.7	1.3
6	$PhCH_2CH_2CH_2$	Ph	75 ± 3	60 ± 5	40 ± 3	121 ± 10	1.9	1.5	3
7	$(CH_3)_2CHCH_2CH_2$	α-naphthyl	142 ± 12	42 ± 3	28 ± 3	215 ± 22	5.07	1.5	7.7
8	$PhCH_2CH_2$	α-naphthyl	90 ± 11	55 ± 6	30 ± 4	120 ± 14	3	1.8	4
9	$PhCH_2CH_2CH_2$	α-naphthyl	1100 ± 100	800 ± 104	20 ± 3	300 ± 28	55	40	15
10	$(CH_3)_2CHCH_2CH_2$	Ph−O	55 ± 5	38 ± 4	25 ± 2	50 ± 5	2.2	1.5	2
11	$PhCH_2CH_2$	Ph−O	20 ± 2	40 ± 3	22 ± 3	300 ± 28	0.9	1.8	13.6
12	$PhCH_2CH_2CH_2$	Ph−O	50 ± 4	45 ± 5	25 ± 4	40 ± 4	2	1.8	1.6

[a] Displacement of specific [^{3}H]-DPCPX binding at human A_1 receptors expressed in CHO cells (n = 3−6). Data are expressed as the mean ± SEM. [b] Displacement of specific [^{3}H]-ZM241385 binding at human A_{2A} receptors expressed in HEK-293 cells. Data are expressed as the mean ± SEM. [c] Displacement of specific [^{3}H]-DPCPX binding at human A_{2B} receptors expressed in HEK-293 cells (n = 3−6). Data are expressed as the mean ± SEM. [d] Displacement of specific [^{3}H]-MRE3008-F20 binding at human A_3 receptors expressed in HEK-293 cells. Data are expressed as the mean ± SEM.

particular, the introduction of an arylacetyl moiety at the N5 position with a concomitant substitution at the N8 position with arylalkyl chains (**5**, **6**) reduces the affinity at the hA_3 adenosine receptors but induces an increase in affinity for the adenosine A_{2B} subtype. It is otherwise noted that when a bulky group such as an α-naphthylacetyl moiety (**4**) was introduced at the N5 position, the selectivity increased in a significant manner (compound **9**: $K_i(hA_1)$ = 1100 nM; $K_i(hA_{2A})$ = 800 nM; $K_i(hA_{2B})$ = 20 nM; $K_i(hA_3)$ = 300 nM; $K_i(hA_1/A_{2B})$ = 55; $K_i(hA_{2A}/A_{2B})$ = 40; $K_i(hA_3/hA_{2B})$ = 15). In particular, this compound represents an example of a slight, potent, and selective non-xanthine A_{2B} adenosine antagonist. An accurate analysis of the data herein presented strongly suggests that a combination of branched (e.g., compounds **4**, **7**, **10**) or arylalkyl (e.g., compounds **5**, **6**, **8**, **9**, **11**, **12**) chains at the N8 position with arylacetyl moieties at the N5 position facilitates the interaction with the A_{2B} adenosine receptors.

The antagonistic properties of the synthesized compounds have been further validated by functional assay, measuring the capability of derivatives **5**−**12** to block the effect of 100 nM NECA on cyclic AMP production to the human A_{2B} adenosine receptors. All the synthesized compounds show IC_{50} values in the nanomolar range (110−250 nM) with a trend similar to that observed in the binding assay (Figure 1 and Table 2).

To elucidate our experimental results, we decided to theoretically compare the putative transmembrane (TM) binding motif of compound **9** on both the hA_{2B} and hA_3 receptors. Following our recently reported modeling approach, we have built an improved model of the transmembrane region of the human A_{2B} receptor, using the rhodopsin crystal structure as template, which can be considered a further refinement in building the hypothetical binding site of the A_{2B} receptor antagonists already proposed.[22] Details of the building model are given in the Experimental Section. Of course, the topology of TM regions of both hA_{2B} and hA_3 is similar,

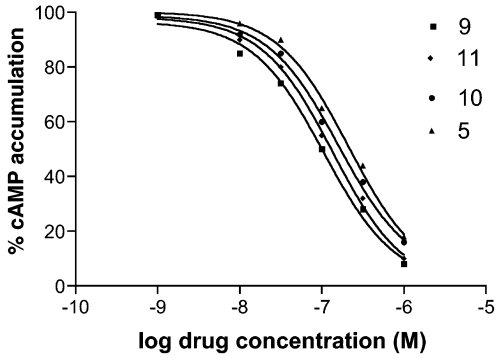

Figure 1. Inhibition curves representing the capability of the antagonists (**5**, **9**−**11**) to block the effect of 100 nM NECA on cyclic AMP production to human A_{2B} adenosine receptors.

Table 2. Functional Assay: IC_{50} Values of Compounds **5**−**12** Examined on 100 nM NECA Stimulation cAMP Accumulation in CHO Cells Expressing hA_{2B} Adenosine Receptors

compd	IC_{50} (nM)
4	190 ± 30
5	210 ± 32
6	250 ± 35
7	170 ± 24
8	180 ± 22
9	110 ± 15
10	150 ± 19
11	130 ± 18
12	140 ± 21

consisting of a typical 3−4 type helix−helix contact associated with optimal interactions between nearly parallel aligned helices. However, by comparison of the TM sequences of both hA_{2B} and hA_3 receptors, several amino acids mutations are detectable in the putative ligand binding cavity. As we will describe later, some of these mutations might play a role in the recognition process of both agonists and antagonists. The first interesting result obtained from our molecular docking studies is that compound **9** can nicely fit inside the TM region of hA_{2B} receptor but not in the hA_3. As already

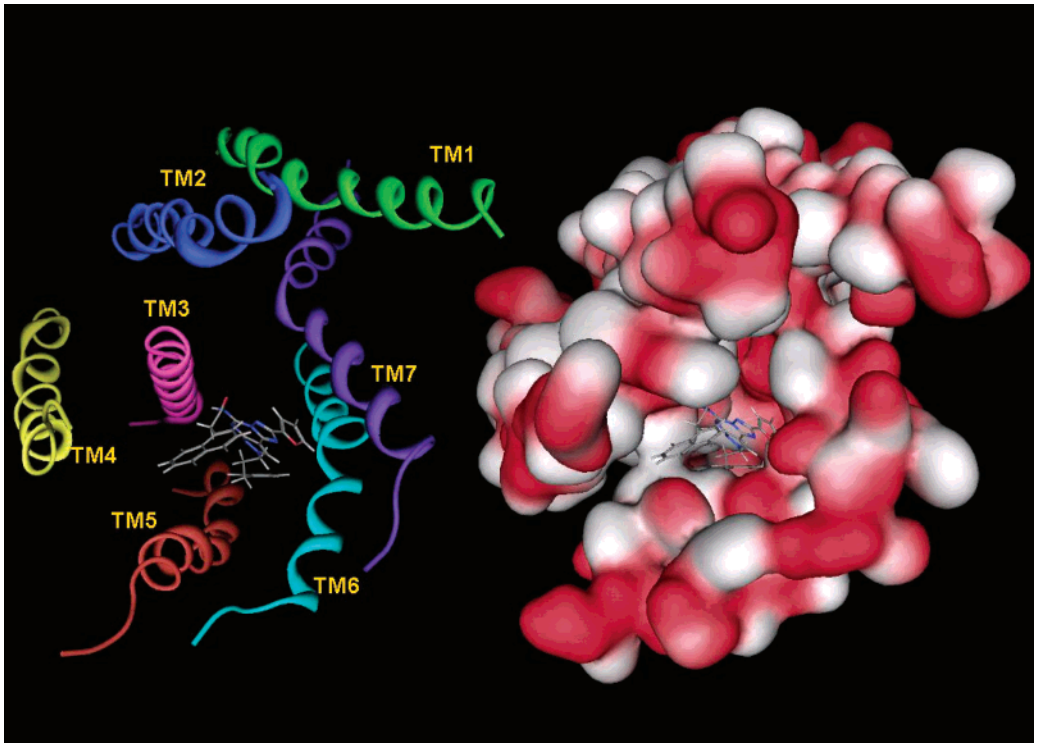

Figure 2. (Left) View hA_{2B} transmembrane helical bundle model along the helical axes from the extracellular end after the docking procedure for the A_{2B}–**9** complex (see Experimental Section for details). The docked **9** molecule is shown. Side chains of some amino acids important for ligand recognition are highlighted. (Right) Molecular surface of A_{2B}–**9** complex model, displayed with MOE. The molecular surface is color-coded by hydrophobicity properties. Hydrophilic regions are red, and hydrophobic regions are white. The ligand is shown in its putative binding site.

indicated, compound **9** bears two bulky groups in both N5 and N8 positions. By analysis of the TM cavity shape of both receptors, it is unambiguous that a deep cleft is present in the hA_{2B} receptor close to TMs 3, 5, and 6, as shown in Figure 2.

The deepness of this cleft is strongly reduced in the hA_3 receptor because of a mutation in TM5 in which Phe187 replaces Leu192 present in the hA_{2B}. The steric hindrance of the phenylalanine side chain is increased with respect to leucine and drastically limited the accessibility to this TM cleft. Interestingly, leucine in position 192 in hA_{2B} is conserved in all adenosine receptor subtypes, but it is mutated to a phenylalanine in the human A_3 receptor. However, in A_1 and A_{2A} receptors, other TM mutations are responsible for the topology modifications of this cleft (data not presented). In the hA_{2B} receptor, we identified the hypothetical binding site of **9** close to TMs 3, 5, and 6, fitting perfectly in this deep cleft, with the furan ring pointing to the extracellular environment. The putative binding site of **9** is shown in Figure 3.

Both the N5 and the N8 side chains are located in two hydrophobic regions. In particular, the 3-(phenyl)-propyl group at the N8 position is surrounded by several hydrophobic amino acids: Ile93 (TM3), Leu96 (TM3), Val191 (TM5), Leu192 (TM5), Leu195 (TM5), Phe243 (TM6), Leu246 (TM6), and Trp247 (TM6). The (α-naphthyl)acetyl group at the N5 position is positioned in the middle of the TM3 and TM5, bordered by Ala82 (TM3), Val87 (TM3), Phe141 (TM4), and Thy184 (TM5). Of course, this deep cleft can also nicely accommodate derivatives in which both the N5 and N8 substituents are smaller than those in compound **9**. In fact, the pyrazolotriazolopyrimidine moiety is located in the middle of the TM cavity, close to TM3 and TM6, and it is stabilized by a hydrogen-bonding interaction with Asn254 (TM6). Also, this amino acid, conserved among all adenosine receptor subtypes, was found to be important for ligand binding. Another hydrogen-bonding interaction between the hydrogen atom of the carboxamido group at the N5 position and the oxygen atom of backbone carboxamido bond of Leu86 might stabilize the position of **9** in its putative binding site.

As anticipated, derivative **9** does not dock in the same way at the hA_3 receptor. In particular, the steric requirements cannot be met because of the restricted topology of hA_3 receptor cleft. The energetically more stable docked configuration is shown in Figure 4.

We identified the hypothetical binding site of **9** close to TMs 2, 3, 6, and 7 in the upper region of TM domain. Considering its bulkiness, compound **9** cannot reach the hydrophilic environment created by Ser 243 (TM6) and Ser 271 (TM7), which are responsible, as we have already published,[23] for the stabilizing interactions with the NH of the phenylcarbamoyl derivatives.

Moreover, both the N5 and N8 side chains are oriented almost perpendicularly to the principal axis of the TM bundle. The 3-(phenyl)propyl group at the N8 position is positioned in the middle of the TM2 and TM7 surrounded by two hydrophobic amino acids: Leu67 (TM2) and Ile270 (TM7). The (α-naphthyl)acetyl group at the N5 position sits in a hydrophobic pocket (corresponding in part to the deep cleft in the A_{2B} receptor) surrounded by Leu91 (TM3) and Leu246 (TM6). Consistent with the experimental data, the theoretically calculated interaction energy of hA_3–**9** complex forma-

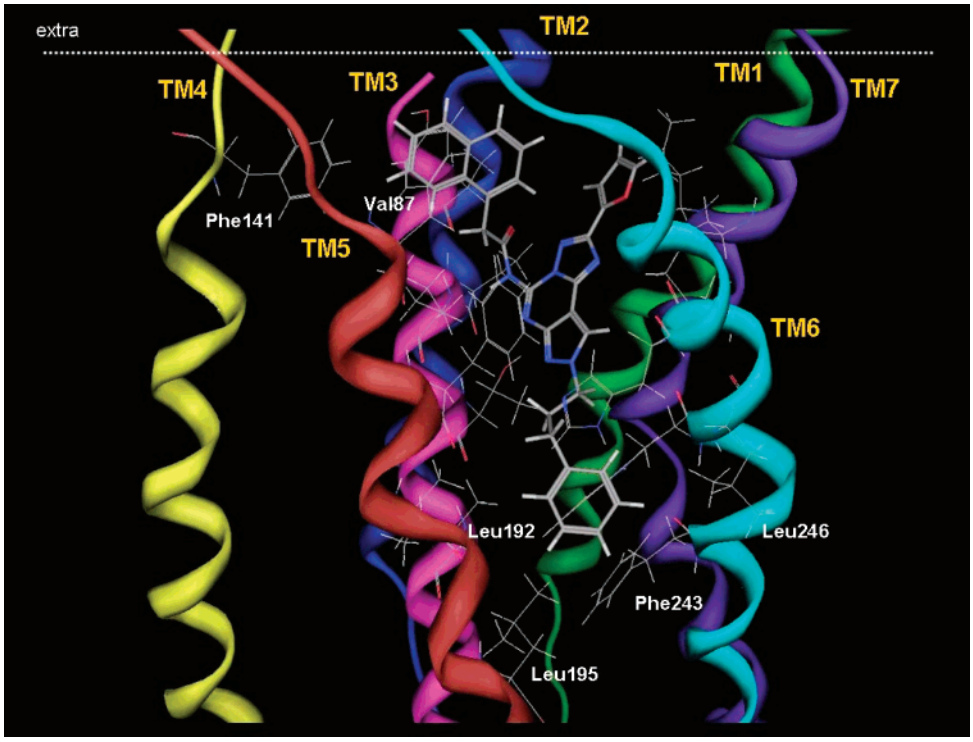

Figure 3. (Left) View of hA_3 transmembrane helical bundle model along the helical axes from the extracellular end after the docking procedure for the A_3–**9** complex (see Experimental Section for details). The docked **9** molecule is shown. Side chains of some amino acids important for ligand recognition are highlighted. (Right) Molecular surface of A_3–**9** complex model, displayed with MOE. The molecular surface is color-coded by hydrophobicity properties. Hydrophilic regions are red, and hydrophobic regions are white. The ligand is shown in its putative binding site.

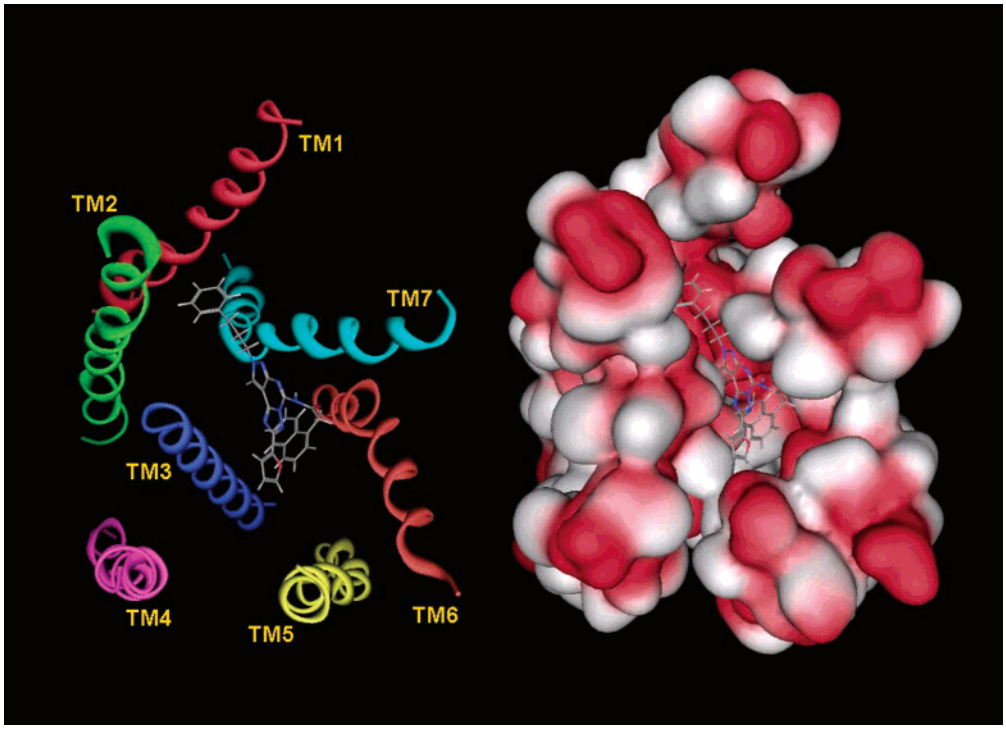

Figure 4. Side view of the A_{2B}–**9** complex model. The side chains of the important residues in proximity (≤4.5 Å) to the docked ligand are highlighted and labeled.

tion is about 55 kcal mol^{-1} higher than that of hA_{2B}–**9** complex formation. (Figure 5).

By comparison of the binding affinity values reported in Table 1, derivative **5** has almost the same potency in both the hA_{2B} and hA_3 adenosine receptors. This compound is characterized by a phenylacetyl at the N5 position and a 2-phenylethyl substitution at the N8 position, and it is less bulky than derivative **9**. To validate our hypothesis about the role of TM steric control on the observed hA_{2B}/hA_3 selectivity, we decided to dock derivative **5** in both receptors. According to our assumption, compound **5** can easily sit in both hA_{2B} and

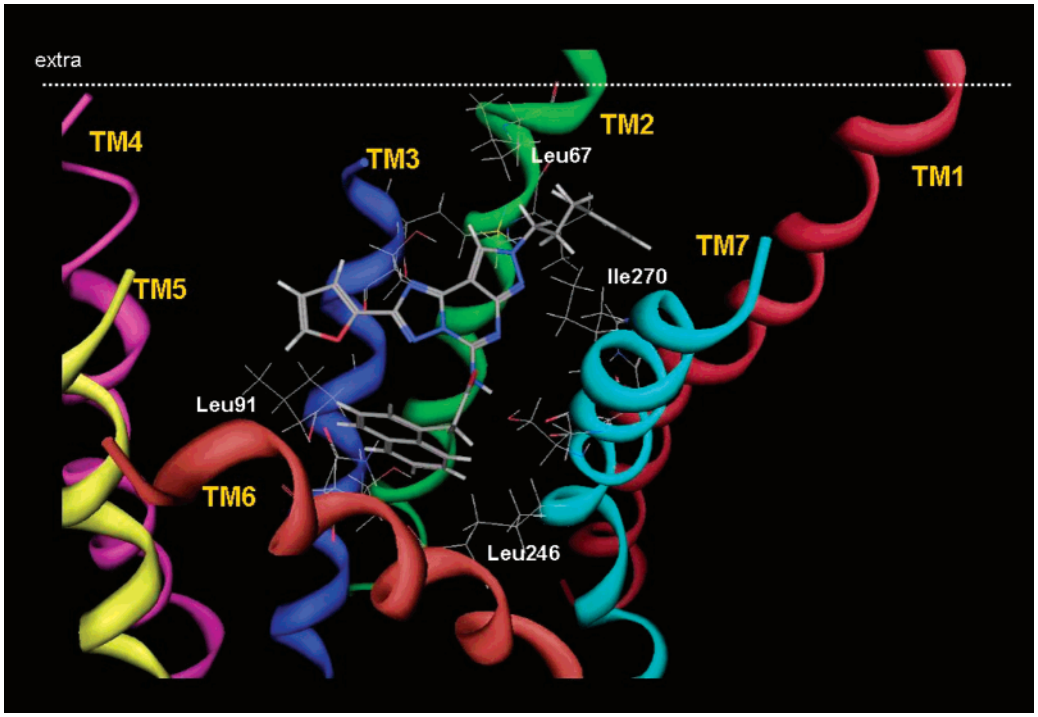

Figure 5. Side view of the A_3−**9** complex model. The side chains of the important residues in proximity (≤4.5 Å) to the docked ligand are highlighted and labeled.

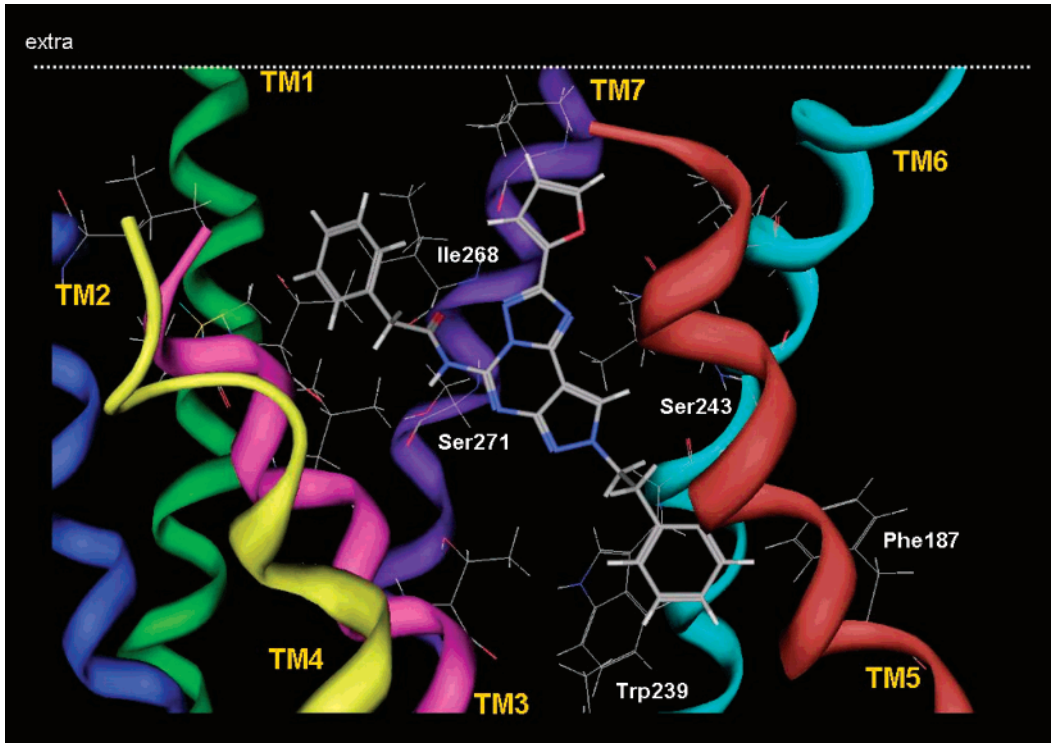

Figure 6. Side view of the A_3−**5** complex model. The side chains of the important residues in proximity (≤4.5 Å) to the docked ligand are highlighted and labeled.

hA_3 adenosine receptors. As shown in Figure 6, considering in particular the complex with the A_3 adenosine receptor, the derivative **5** arrangement is consistent with the recently published model of the putative binding motif of the pyrazolotriazolopyrimidines bearing a urea moiety at the N5 position.[23]

On the basis of this information, we have already suggested that the hydrophilic environment created by Ser243 (TM6) and Ser271 (TM7) in the human A_3 receptor might be responsible for the better accommodation of the phenylcarbamoyl NH into the hypothesized binding site with respect to the CH_2 of the arylacetyl derivatives.

The well-known mutation[21] of Ser243 (TM6) to a hystidine in all other adenosine receptor subtypes might be responsible for the peculiar selectivity observed for the phenylcarbamoyl derivatives at the human A_3 receptor.

Considering the binding motif of compound **5**, we identified its hypothetical binding site close to TMs 3, 6, and 7 with the furan ring pointing to the extracellular environment. The most stabilizing interactions are (a) the hydrogen bonds between the NH in the N5 position and the hydroxyl group of Ser243, (b) the hydrophobic interactions of the phenylacetyl in the N5 position with the hydrophobic side chains of Met86 (TM3), Leu90 (TM3), and Ile268 (TM7), and (c) the hydrophobic interactions of the 2-phenylethyl substitution at the N8 position with Phe187 (TM5) and Trp239 (TM6).

Conclusions

The present study provides useful information concerning the optimal structural requirements necessary for antagonist recognition of the hA_{2B} adenosine receptor. It demonstrates that probably bulky groups at the N5 and N8 positions on the pyrazolotriazolopyrimidine core confer a slightly better affinity for the A_{2B} adenosine receptor subtype with respect to the other receptor subtypes. By the use of molecular modeling, the differences in interaction between this class of compounds and the hA_{2B} and A_3 receptors have been clarified: (a) Considering the topological differences in the TM cavity between hA_{2B} and hA_3 adenosine receptors, bulky substituents at both the N5 and N8 positions are well tolerated at the hA_{2B} adenosine receptor only if an acetyl moiety is present at the N5 position. (b) Bulky substituents at both the N5 and N8 positions are not well tolerated at the hA_3 adenosine receptor. (c) In the hA_3 receptor, the hydrophilic environment created by Ser243 (TM6) and Ser271 (TM7) might be responsible for the better accommodation of the NH of the phenylcarbamoyl derivatives in the hypothetical binding site with respect to the CH_2 present in the phenylacetyl derivatives.

In conclusion, the data herein presented provide helpful information for designing new, more potent and selective hA_{2B} adenosine receptor antagonists.

Experimental Section

1. Chemistry. General. Reactions were routinely monitored by thin-layer chromatography (TLC) on silica gel (precoated F_{254} Merck plates). Infrared spectra (IR) were measured on a Jasco FT-IR instrument. ^{1}H NMR were determined in $CDCl_3$ or DMSO-d_6 solutions with a Varian Gemini 200 spectrometer. Peaks positions are given in parts per million (δ) downfield from tetramethylsilane as the internal standard, and J values are given in hertz. Light petroleum ether refers to the fractions boiling at 40−60 °C. Melting points were determined on a Buchi-Tottoli instrument and are uncorrected. Flash chromatograpy was performed using Merck 60−200 mesh silica gel. Elemental analyses were performed by the microanalytical laboratory of Dipartimento di Chimica, University of Trieste, and were within ±0.4% of the theoretical values for C, H, and N.

General Procedures for the Preparation of 5-[(Aryl)-carbonyl]amino-8-(ar)alkyl-2-(2-furyl)pyrazolo[4,3-*e*]-1,2,4-triazolo[1,5-*c*]pyrimidine (4−12). The compounds were prepared as described in the literature.[23]

5-[(Benzyl)carbonyl]amino-8-isopentyl-2-(2-furyl)pyrazolo[4,3-*e*]-1,2,4-triazolo[1,5-*c*]pyrimidine (4). Yield 85%, pale-yellow solid (EtOAc−light petroleum), mp 144−145 °C. IR (KBr): 3255−2930, 1673, 1620, 1610, 1520 cm^{-1}. ^{1}H NMR ($CDCl_3$) δ: 0.98 (d, 6H, J = 7.5 Hz), 1.60 (m, 1H), 1.91 (m, 2H), 4.40 (t, 2H, J = 7 Hz), 4.53 (s, 2H), 6.60 (dd, 1H, J = 2 Hz, J = 4 Hz), 7.18 (d, 1H, J = 4 Hz), 7.26−7.39 (m, 5H), 7.64 (d, 1H, J = 2 Hz), 8.22 (s, 1H), 9.11 (bs, 1H). Anal. ($C_{23}H_{23}N_7O_2$) C, H, N.

5-[(Benzyl)carbonyl]amino-8-(2-phenylethyl)-2-(2-furyl)-pyrazolo[4,3-*e*]-1,2,4-triazolo[1,5-*c*]pyrimidine (5). Yield 80%, white solid (EtOAc−light petroleum), mp 147 °C. IR (KBr): 3240−2920, 1673, 1614, 1600, 1505 cm^{-1}. ^{1}H NMR ($CDCl_3$) δ: 3.21 (t, 2H, J = 7 Hz), 3.98 (s, 2H), 4.61 (t, 2H, J = 7 Hz), 6.65 (dd, 1H, J = 2 Hz, J = 4 Hz), 7.05−7.45 (m, 11H), 7.98 (d, 1H, J = 4 Hz), 8.67 (s, 1H), 11.12 (bs, 1H). Anal. ($C_{26}H_{21}N_7O_2$) C, H, N.

5-[(Benzyl)carbonyl]amino-8-(3-phenylpropyl)-2-(2-furyl)pyrazolo[4,3-*e*]-1,2,4-triazolo[1,5-*c*]pyrimidine (6). Yield 85%, pale-yellow solid (EtOAc−light petroleum), mp 116−117 °C. IR (KBr): 3250−2900, 1675, 1625, 1600, 1500 cm^{-1}. ^{1}H NMR ($CDCl_3$) δ: 2.39 (m, 2H), 2.67 (t, 2H, J = 7 Hz), 4.37 (t, 2H, J = 7 Hz), 4.53 (s, 2H), 6.61 (dd, 1H, J = 2 Hz, J = 4 Hz), 7.16−7.43 (m, 11H), 7.65 (d, 1H, J = 4 Hz), 7.64 (s, 1H), 8.19 (s, 1H), 9.12 (bs, 1H). Anal. ($C_{27}H_{23}N_7O_2$) C, H, N.

5-[(α-Naphthylmethyl)carbonyl]amino-8-isopentyl-2-(2-furyl)pyrazolo[4,3-*e*]-1,2,4-triazolo[1,5-*c*]pyrimidine (7). Yield 80%, pale-yellow solid (EtOAc−light petroleum), mp 95−96 °C. IR (KBr): 3240−2950, 1680, 1625, 1595, 1510 cm^{-1}. ^{1}H NMR ($CDCl_3$) δ: 0.97 (d, 6H, J = 7.5 Hz), 1.47−1.50 (m, 1H), 1.83−1.95 (m, 2H), 4.40 (t, 2H, J = 7 Hz), 4.59 (s, 2H), 6.67 (dd, 1H, J = 2 Hz, J = 4 Hz), 7.19 (d, 1H, J = 4 Hz), 7.21−7.59 (m, 4H), 7.79−8.15 (m, 4H), 8.81 (s, 1H), 11.03 (bs, 1H). Anal. ($C_{27}H_{25}N_7O_2$) C, H, N.

5-[(α-Naphthylmethyl)carbonyl]amino-8-(2-phenylethyl)-2-(2-furyl)pyrazolo[4,3-*e*]-1,2,4-triazolo[1,5-*c*]pyrimidine (8). Yield 74%, white solid (EtOAc−light petroleum), mp 107 °C. IR (KBr): 3250−2970, 1678, 1620, 1595, 1500 cm^{-1}. ^{1}H NMR ($CDCl_3$) δ: 3.12 (t, 2H, J = 7 Hz), 4.41 (s, 2H), 4.61 (t, 2H, J = 7 Hz), 6.64 (dd, 1H, J = 2 Hz, J = 4 Hz), 7.03−7.15 (m, 5H), 7.25−7.39 (m, 4H), 7.81−8.00 (m, 4H), 8.03 (d, 1H, J = 4 Hz), 8.82 (s, 1H), 11.03 (bs, 1H). Anal. ($C_{30}H_{23}N_7O_2$) C, H, N.

5-[(α-Naphthylmethyl)carbonyl]amino-8-(3-phenylpropyl)-2-(2-furyl)pyrazolo[4,3-*e*]-1,2,4-triazolo[1,5-*c*]pyrimidine (9). Yield 82%, pale-yellow solid (EtOAc−light petroleum), mp 109 °C. IR (KBr): 3240−2980, 1676, 1610, 1585, 1510 cm^{-1}. ^{1}H NMR ($CDCl_3$) δ: 2.15 (t, 2H, J = 7 Hz), 2.65−2.78 (m, 2H), 4.38 (t, 2H, J = 7 Hz), 4.44 (s, 2H), 4.61 (t, 2H, J = 7 Hz), 6.67 (dd, 1H, J = 2 Hz, J = 4 Hz), 7.03−7.18 (m, 5H), 7.32−7.59 (m, 4H), 7.65−8.11 (m, 5H), 8.92 (s, 1H), 11.10 (bs, 1H). Anal. ($C_{31}H_{25}N_7O_2$) C, H, N.

5-[(Phenoxymethyl)carbonyl]amino-8-isopentyl-2-(2-furyl)pyrazolo[4,3-e]-1,2,4-triazolo[1,5-*c*]pyrimidine (10). Yield 80%, white solid (EtOAc−light petroleum), mp 175 °C. IR (KBr): 3235−2960, 1675, 1620, 1595, 1515 cm^{-1}. ^{1}H NMR ($CDCl_3$) δ: 0.98 (d, 6H, J = 7.5 Hz), 1.39−1.45 (m, 1H), 1.88−1.97 (m, 2H), 4.41 (t, 2H, J = 7 Hz), 5.04 (s, 2H), 6.75 (dd, 1H, J = 2 Hz, J = 4 Hz), 6.95−7.08 (m, 3H), 7.19−7.40 (m, 3H), 7.96 (d, 1H, J = 2 Hz), 8.88 (s, 1H), 10.98 (bs, 1H). Anal. ($C_{23}H_{25}N_7O_3$) C, H, N.

5-[(Phenoxymethyl)carbonyl]amino-8-(2-phenylethyl)-2-(2-furyl)pyrazolo[4,3-*e*]-1,2,4-triazolo[1,5-*c*]pyrimidine (11). Yield 68%, brown solid (EtOAc−light petroleum), mp 107 °C. IR (KBr): 3245−2980, 1670, 1615, 1590, 1515 cm^{-1}. ^{1}H NMR ($CDCl_3$) δ: 3.46 (t, 2H, J = 7 Hz), 4.52 (t, 2H, J = 7 Hz), 5.05 (s, 2H), 6.72 (dd, 1H, J = 2 Hz, J = 4 Hz), 6.81−7.47 (m, 11H), 7.95 (d, 1H, J = 2 Hz), 8.88 (s, 1H), 10.96 (bs, 1H). Anal. ($C_{26}H_{21}N_7O_3$) C, H, N.

5-[(Phenoxymethyl)carbonyl]amino-8-(3-phenylpropyl)-2-(2-furyl)pyrazolo[4,3-*e*]-1,2,4-triazolo[1,5-*c*]pyrimidine (12). Yield 72%, brown solid (EtOAc−light petroleum), mp 85 °C. IR (KBr): 3230−2985, 1681, 1615, 1590, 1510 cm^{-1}. ^{1}H NMR ($CDCl_3$) δ: 2.19 (t, 2H, J = 7 Hz), 2.61−2.73 (m, 2H), 4.27 (t, 2H, J = 7 Hz), 5.04 (s, 2H), 6.61 (dd, 1H, J = 2 Hz, J = 4 Hz), 6.81−7.43 (m, 11H), 7.65 (d, 1H, J = 4 Hz), 8.23 (s, 1H), 10.02 (bs, 1H). Anal. ($C_{27}H_{25}N_7O_3$) C, H, N.

2. Biology. 2.1. CHO Membrane Preparation. The expression of the human A_1, A_{2A}, and A_3 receptors in CHO cells has been previously described.[31] The cells were grown adherently and maintained in Dulbecco's modified Eagle's medium with nutrient mixture F12 without nucleosides at 37 °C in 5% CO_2/95% air. Cells were split two or three times weekly, and

then the culture medium was removed for membrane preparations. The cells were washed with phosphate-buffered saline solution and were scraped from flasks in ice-cold hypotonic buffer (5 mM Tris-HCl, 2 mM EDTA, pH 7.4). The cell suspension was homogenized with Polytron, and the homogenate was centrifuged for 30 min at 48000*g*. The membrane pellet was resuspended in 50 mM Tris-HCl buffer at pH 7.4 for A_1 adenosine receptors, in 50 mM Tris-HCl, 10 mM $MgCl_2$ at pH 7.4 for A_{2A} adenosine receptors, and in 50 mM Tris-HCl, 10 mM $MgCl_2$, 1 mM EDTA at pH 7.4 for A_3 adenosine receptors and were utilized for binding assay.

2.2. Human Cloned A_1, A_{2A}, A_{2B}, and A_3 Adenosine Receptor Binding Assay. Binding of [^{3}H]-DPCPX to CHO cells transfected with the human recombinant A_1 adenosine receptor was performed as previously described.[28] Displacement experiments were performed for 120 min at 25 °C in 0.20 mL of buffer containing 1 nM [^{3}H]-DPCPX, 20 μL of diluted membranes (50 μg of protein/assay) and at least six to eight different concentrations of examined compounds. Nonspecific binding was determined in the presence of 10 μM of CHA, and this is always ≤10% of the total binding. Binding of [^{3}H]-ZM241385 to CHO cells transfected with the human recombinant A_{2A} adenosine receptors (50 μg of protein/assay) was performed according to Ongini et al.[30] In competition studies, at least six to eight different concentrations of compounds were used and nonspecific binding was determined in the presence of 50 μM NECA for an incubation time of 60 min at 25 °C.

Binding of [^{3}H]-DPCPX to HEK-293 cells (Receptor Biology Inc., Beltsville, MD) transfected with the human recombinant A_{2B} adenosine receptors was performed as already described.[29] In particular, assays were carried out for 60 min at 25 °C in 0.1 mL of 50 mM Tris-HCl buffer, 10 mM $MgCl_2$, 1 mM EDTA, 0.1 mM benzamidine, pH 7.4, 2 IU/mL adenosine deaminase containing 40 nM [^{3}H]-DPCPX, diluted membranes (20 μg of protein/assay), and at least six to eight different concentrations of tested compounds. Nonspecific binding was determined in the presence of 100 μM of NECA and was always ≤30% of the total binding. Binding of [^{3}H]-MRE3008-F20 to CHO cells transfected with the human recombinant A_3 adenosine receptors was performed according to Varani et al.[29] Competition experiments were carried out in duplicate in a finale volume of 250 μL in test tubes containing 1 nM [^{3}H]-MRE3008-F20, 50 mM Tris-HCl buffer, 10 mM $MgCl_2$, pH 7.4, 100 μL of diluted membranes (50 μg of protein/assay), and at least six to eight different concentrations of examined ligands. Incubation time was 120 min at 4 °C, according to the results of previous time-course experiments.[29] Nonspecific binding was defined as binding in the presence of 1 μM MRE3008-F20 and was about 25% of the total binding. Bound and free radioactivity was separated by filtering the assay mixture through Whatman GF/B glass-fiber filters using a Micro-Mate 196-cell harvester (Packard Instrument Company). The filter bound radioactivity was counted on Top Count (efficiency of 57%) with Micro-Scint 20. The protein concentration was determined according to the Bio-Rad method[32] with bovine albumin as a reference standard.

2.3. Measurement of Cyclic AMP Levels in CHO Cells Transfected with Human A_{2B} Adenosine Receptors. CHO cells transfected with human A_{2B} adenosine receptors were washed with phosphate-buffered saline and diluted tripsine and centrifuged for 10 min at 200*g*. The pellet containing the CHO cells (1×10^6 cells/assay) was suspended in 0.5 mL of incubation mixture (mM): NaCl 15, KCl 0.27, NaH_2PO_4 0.037, $MgSO_4$ 0.1, $CaCl_2$ 0.1, Hepes 0.01, $MgCl_2$ 1, glucose 0.5, pH 7.4 at 37 °C, 2 IU/mL adenosine deaminase, and 4-(3-butoxy-4-methoxybenzyl)-2-imidazolidinone (Ro 20-1724) as phosphodiesterase inhibitor. The mixture was preincubated for 10 min in a shaking bath at 37 °C. The potency of antagonists studied was determined by antagonism of NECA (100 nM) induced stimulation of cyclic AMP levels. The reaction was terminated by the addition of cold 6% trichloroacetic acid (TCA). The TCA suspension was centrifuged at 2000*g* for 10 min at 4 °C, and the supernatant was extracted four times with water-saturated diethyl ether. The final aqueous solution was tested for cyclic AMP levels by a competition protein binding assay. Samples of cyclic AMP standard (0−10 pmol) were added to each test tube containing the incubation buffer (trizma base 0.1 M, aminophylline 8.0 mM, 2 mercaptoethanol 6.0 mM, pH 7.4) and [^{3}H]-cyclic-AMP in a total volume of 0.5 mL. The binding protein previously prepared from beef adrenals was added to the samples previously incubated at 4 °C for 150 min, and after the addition of charcoal, the samples were centrifuged at 2000*g* for 10 min. The clear supernatant was counted in a Beckman scintillation counter.

3. Molecular Modeling. All calculations were performed on a Silicon Graphics Octane R12000 workstation.

Human A_{2B} and A_3 receptor models were built and optimized using the MOE (2002.03) modeling package[33] based on the approach described by Moro et al.[34] Briefly, transmembrane domains were identified with the aid of Kyte−Doolittle hydrophobicity and E_{min} surface probability parameters.[35] Transmembrane helices were built from the sequences and minimized individually. The minimized helices were then grouped together to form a helical bundle matching the overall characteristics of the recently published crystal structure of bovine rhodopsin (PDB code: 1F88).[36] The helical bundle was minimized using the Amber94 force field[37] until the root mean square (rms) value of the conjugate gradient (CG) was <0.01 kcal mol^{-1} Å^{-1}. A fixed dielectric constant of 4.0 was used throughout these calculations. In the final step, the stereochemical quality of the models were checked with the "Protein Report", "Ramachandran Plot", and "Chi Plot" modules implemented in MOE.

All docked derivatives were fully optimized without geometry constraints using RHF/AM1 semiempirical calculations. Vibrational frequency analyses were used to characterize the minimal stationary points (zero imaginary frequencies). The software package Spartan O2 was utilized for all quantum mechanical calculations.[38]

The ligands were docked into the hypothetical TM binding site by using the DOCK docking program, part of the MOE suite. Searching is conducted within a user-specified 3D docking box, using the Tabù Search protocol[39] and MMFF94 force field.[40−46] MOE-Dock performs a user-specified number of independent docking runs (50 in our specific case) and writes the resulting conformations and their energies to a molecular database file. The resulting docked complexes were subjected to MMFF94 energy minimization until the rms of the conjugate gradient was <0.1 kcal mol^{-1} Å^{-1}. Charges for the ligands were imported from the Spartan output files.

The interaction energy values were calculated as follows: $\Delta E_{binding} = E_{complex} - (E_{ligand} + E_{receptor})$. These energies are not rigorous thermodynamic quantities but can only be used to compare the relative stabilities of the complexes. Consequently, these interaction energy values cannot be used to calculate binding affinities because changes in entropy and solvation effects are not taken into account.

Acknowledgment. We thank the Regione Friuli Venezia Giulia (Fondo 2000) and the University of Trieste (fondo 60%) for financial support.

Appendix

Abbreviations. NECA, 5′-(*N*-ethylcarbamoyl)adenosine; CHA, N^6-cyclohexyladenosine; DPCPX, 8-cyclopentyl-1,3-dipropylxanthine; DMSO, dimethyl sulfoxide; THF, tetrahydrofuran; CHO cells, Chinese hamster ovary cells; HEK cells, human embryonic kidney cells; MRE3008-F20, 5-(((4-methoxyphenyl)amino)carbonyl)-amino-8-propyl-2-(2-furyl)pyrazolo[4,3-*e*]-1,2,4-triazolo-[1,5-*c*]pyrimidine; EtOAc, ethyl acetate; TLC, thin-layer chromatography; ZM 241385, (4-[2-[[7-amino-2-(2-furyl)-1,2,4-triazolo[2,3-*a*]-1,3,5-triazin-5-yl]amino]ethyl]phenol); mp, melting point; NMR, nuclear magnetic resonance; IR, infrared spectra; $CHCl_3$, chloroform; EDTA, ethylenediaminetetraacetic acid.

References

(1) Fredholm, B. B.; Ijzerman, A. P.; Jacobson, K. A.; Klotz, K. N.; Linden, J. International Union of Pharmacology. XXV. Nomenclature and classification of adenosine receptors. *Pharmacol. Rev.* **2001**, *53*, 527−552.

(2) Jacobson, K. A.; Knutsen, L. J. S. P1 and P2 purine and pyrimidine receptor ligands. In *Purinergic and Pyrimidinergic Signalling*; Abbracchio, M. P., Williams, M., Eds.; Handbook of Experimental Pharmacology, Vol. 151/1; Springer: Berlin, 2001; pp 129−175.

(3) Ralevic, V.; Burnstock, G. Receptors for purines and pyrimidines. *Pharmacol. Rev.* **1998**, *50*, 413−492.

(4) Baraldi, P. G.; Cacciari, B.; Romagnoli, R.; Merighi, S.; Varani, K.; Borea, P. A.; Spalluto, G. A_3 Adenosine receptor ligands; history and perspectives. *Med. Res. Rev.* **2000**, *20*, 103−128.

(5) Feoktistov, I.; Biaggioni, I. Adenosine A_{2B} receptors. *Pharmacol. Rev.* **1997**, *49*, 381−402.

(6) Volpini, R.; Costanzi, S.; Vittori, S.; Cristalli, G.; Klotz, K. N. Medicinal chemistry and pharmacology of A_{2B} adenosine receptors. *Curr. Top. Med. Chem.* **2003**, *3*, 427−443.

(7) Feoktistov, I.; Biaggioni, I. Pharmacological characterization of adenosine A_{2B} receptors. *Biochem. Pharmacol.* **1998**, *55*, 627−633.

(8) Feoktistov, I.; Biaggioni, I. Adenosine A_{2B} receptors evoke interleukine-S secretion in human mast cells: an enprofylline-sensitive mechanism with implication for asthma. *J. Clin. Invest.* **1995**, *96*, 1979−1986.

(9) Linden, J.; Figler, R. A.; Wang, G.; Jones, D. R.; Jacobson, K. A.; LaNoue, K. F. A_{2B} adenosine receptor antagonists for asthma and diabetes. Presented at the 224th National Meeting of the American Chemical Society, Boston, MA, August 18−22, 2002; Paper MEDI-418.

(10) Boyle, D. L.; Sajjadi, F. G.; Firestein, G. S. Inhibition of synoviocyte collagenase gene expression by adenosine receptor stimulation. *Arthritis Rheum.* **1996**, *39*, 923−930.

(11) Dubey, R. K.; Gillaspie, D. G.; Osaka, K.; Suzuki, F.; Jackson, E. K. Adenosine inhibits growth of rat aortic smooth muscle cells: possible role of A_{2B} receptors. *Hypertension* **1996**, *27*, 786−793.

(12) Murthy, K. S.; McHenry, L.; Grider, J. R.; Makhlouf, G. M. Adenosine A_1 and A_{2B} receptors coupled to distinct interactive signaling pathways in intestinal muscle cells. *J. Pharmacol. Exp. Ther.* **1995**, *274*, 243−246.

(13) Rubino, A.; Ralevic, V.; Burnstock, G. Contribution of P1 (A_{2B}-subtype) and P2-purinoceptors to the control of vascular tone in the rat isolate mesenteric arterial bed. *Br. J. Pharmacol.* **1995**, *115*, 648−652.

(14) Feoktistov, I.; Wells, J. N.; Biaggioni, I. Adenosine A_{2B} receptors as therapeutic targets. *Drug Dev. Res.* **1998**, *45*, 198−206.

(15) Jacobson, K. A.; Ijzerman, A. P.; Linden, J. 1,3-Dialkylxanthine derivatives having high potency as antagonists at human A_{2B} adenosine receptors. *Drug Dev. Res.* **1999**, *47*, 45−53.

(16) Kim, Y.-C.; Karton, Y.; Ji, X.-D.; Melman, N.; Linden, J.; Jacobson, K. A. Acyl-hydrazide derivatives of a xanthine carboxylic congener (XCC) as selective antagonists at human A_{2B} adenosine receptors. *Drug Dev. Res.* **1999**, *47*, 178−188.

(17) Kim, Y.-C.; Ji, X.-D.; Melman, N.; Linden, J.; Jacobson, K. A. Anilide derivatives of an 8-phenylxanthine carboxylic congener are highly potent and selective antagonists at human A_{2B} adenosine receptors. *J. Med. Chem.* **2000**, *43*, 1165−1172.

(18) Hayallah, A. M.; Sandoval-Ramirez, J.; Reith, U.; Schobert, U.; Preiss, B.; Schumacher, B.; Daly, J. W.; Muller, C. E. 1,8-Disubstituted xanthine derivatives: synthesis of potent A_{2B}-selective adenosine receptor antagonists. *J. Med. Chem.* **2002**, *45*, 1500−1510.

(19) Kim, S. A.; Marshall, M. A.; Melman, N.; Kim, S. H.; Muller, C. E.; Linden, J.; Jacobson, K. A. Structure−activity relationships at human and rat adenosine receptors of xanthine derivatives substituted at the 1-, 3-, 7-, and 8-positions. *J. Med. Chem.* **2002**, *45*, 2131−2138.

(20) deZwart, M.; Vollinga, R. C.; Beukers, M. W.; Sleegers, D. F.; von Frijtag Drabbe Kunzel, J. K.; de Groote, M.; Ijzerman, A. P. Potent antagonist for the human adenosine A_{2B} receptor. Derivatives of the triazolotriazine adenosine receptor antagonist ZM241385 with high affinity. *Drug Dev. Res.* **1999**, *48*, 95−103.

(21) Kim, Y. C.; de Zwart, M.; Chang, L.; Moro, S.; Jacobien, K.; Frijtag, D. K.; Melman, N.; IJzerman, A. P.; Jacobson, K. A. Derivatives of the triazoloquinazoline adenosine antagonist (CGS15943) having high potency at the human A_{2B} and A_3 receptor subtypes. *J. Med. Chem.* **1998**, *41*, 2835−2845.

(22) Webb, T. R.; Lvovskiy, D.; Kim, S.-A.; Ji, X.-D.; Melman, N.; Linden, J.; Jacobson, K. A. Quinazolines as adenosine receptor antagonists: SAR and selectivity for A_{2B} receptors. *Bioorg. Med. Chem.* **2003**, *11*, 77−85.

(23) Baraldi, P. G.; Cacciari, B.; Moro, S.; Spalluto, G.; Pastorin, G.; Da Ros, T.; Klotz, K.-N.; Varani, K.; Gessi, S.; Borea, P. A. Synthesis, Biological Activity, and Molecular Modeling Investigation of New Pyrazolo[4,3-*e*]1,2,4-triazolo[1,5-*c*]pyrimidine Derivatives as Human A_3 Adenosine Receptor Antagonists. *J. Med. Chem.* **2002**, *45*, 770−780.

(24) Baraldi, P. G.; Cacciari, B.; Romagnoli, R.; Klotz, K. N.; Spalluto, G.; Varani, K.; Gessi, S.; Merighi, S.; Borea, P. A. Pyrazolo[4,3-*e*]1,2,4-triazolo[1,5-*c*]pyrimidine derivatives as adenosine receptor ligands: A starting point for searching A_{2B} adenosine receptor antagonists. *Drug Dev. Res.* **2001**, *53*, 225−235.

(25) Baraldi, P. G.; Cacciari, B.; Romagnoli, R.; Spalluto, G.; Klotz, K.-N.; Leung, E.; Varani, K.; Gessi, S.; Merighi, S.; Borea, P. A. Pyrazolo[4,3-*e*]1,2,4-triazolo[1,5-*c*]pyrimidine derivatives as highly potent and selective human A_3 adenosine receptor antagonists. *J. Med. Chem.* **1999**, *42*, 4473−4478.

(26) Baraldi, P. G.; Cacciari, B.; Romagnoli, R.; Spalluto, G.; Moro, S.; Klotz, K. N.; Leung, E.; Varani, K.; Gessi, S.; Merighi, S.; Borea, P. A. Pyrazolo[4,3-*e*]1,2,4-triazolo[1,5-*c*]pyrimidine derivatives as highly potent and selective human A_3 adenosine receptor antagonists: Influence of the chain at N^8 pyrazole nitrogen. *J. Med. Chem.* **2000**, *43*, 4768−4780.

(27) Baraldi, P. G.; Caccairi, B.; Romagnoli, R.; Moro, S.; Ji, X.-D.; Jacobson, K. A.; Gessi, S.; Borea, P. A.; Spalluto, G. Fluorosulfonyl- and bis-(β-chloroethyl)amino-phenyl functionalized pyrazolo[4,3-*e*]1,2,4-triazolo[1,5-*c*]pyrimidine derivatives as irreversible antagonists at the human A_3 adenosine receptor: molecular modeling studies. *J. Med. Chem.* **2001**, *44*, 2735−2742.

(28) Lohse, M. J.; Klotz, K.-N.; Lindernborn-Fotinos, J.; Reddington, M.; Schwabe, U.; Olsson, R. A. 8-Cyclopentyl 1,3-dipropylxanthine DPCPX a selective high affinity antagonist radioligand for A_1 adenosine receptors. *Naunyn-Schmiedeberg's Arch. Pharmacol.* **1987**, *336*, 204−210.

(29) Varani, K.; Merighi, S.; Gessi, S.; Klotz, K. N.; Leung, E.; Baraldi, P. G.; Cacciari, B.; Spalluto, G.; Borea, P. A. [^{3}H]MRE3008-F20: a novel antagonist radioligand for the pharmacological and biochemical characterization of human A_3 adenosine receptors. *Mol. Pharmacol.* **2000**, *57*, 968−975.

(30) Ongini, E.; Dionisotti, S.; Gessi, S.; Irenius, E.; Fredholm, B. B. Comparison of CGS 15943 and SCH 58261 as antagonist at human A_3 adenosine receptors. *Naunyn Schmiedeberg's Arch. Pharmacol.* **1999**, *359*, 7−10.

(31) Klotz, K. N.; Hessling, J.; Hegler, J.; Owman, C.; Kull, B.; Fredholm, B. B.; Lohse, M. J. Comparative pharmacology of human adenosine receptor subtypes—characterization of stably transfected receptors in CHO cells. *Naunyn-Schmiedeberg's Arch. Pharmacol.* **1998**, *357*, 1−9.

(32) Bradford, M. M. A rapid sensitive method for the quantification of microgram quantities of protein utilizing the principle of protein dye-binding. *Anal. Biochem.* **1976**, *72*, 248−254.

(33) Molecular Operating Environment (MOE 2002.03): Chemical Computing Group, Inc., 1255 University Street, Suite 1600, Montreal, Quebec, H3B 3X3, Canada.

(34) Moro, S.; Guo, D.; Camaioni, E.; Boyer, J. L.; Harden, K. T.; Jacobson, K. A. Human $P2Y_1$ receptor: molecular modeling and site-directed mutagenesis as tools to identify agonist and antagonist recognition sites. *J. Med. Chem.* **1998**, *41*, 1456−1466.

(35) Kyte, J.; Doolittle, R. F. A simple method for displaying the hydrophobic character of a protein. *J. Mol. Biol.* **1982**, *157*, 105−132.

(36) Palczewski, K.; Kumasaka, T.; Hori, T.; Behnke, C. A.; Motoshima, H.; Fox, B. A.; Le Trong, I.; Teller, D. C.; Okada, T.; Stenkamp, R. E.; Yamamoto, M.; Miyano, M. Crystal Structure of Rhodopsin: A G Protein-Coupled Receptor. *Science* **2000**, *289*, 739−745.

(37) Cornell, W. D.; Cieplak, P.; Bayly, C. I.; Gould, I. R.; Merz, K. M.; Ferguson, D. M.; Spellmeyer, D. C.; Fox, T.; Caldwell, J. W.; Kollman, P. A. A Second Generation Force Field for the Simulation of Proteins, Nucleic Acids, and Organic Molecules. *J. Am. Chem. Soc.* **1995**, *117*, 5179−5196.

(38) Spartan O2: Wavefuncion Inc., 18401 Von Karman Avenue, Irvine, CA 92612.

(39) Baxter, C. A.; Murray, C. W.; Clark, D. E.; Westhead, D. R.; Eldridge, M. D. Flexible Docking Using Tabu Search and an Empirical Estimate of Binding Affinity. *Proteins: Struct., Funct., Genet.* **1998**, *33*, 367−382.

(40) Halgren, T. A. Merck Molecular Force Field. I. Basis, Form, Scope, Parameterization, and Performance of MMFF94. *J. Comput. Chem.* **1996**, *17*, 490−519.

(41) Halgren, T. A. Merck Molecular Force Field. II. MMFF94 van der Waals and Electrostatic Parameters for Intermolecular Interactions. *J. Comput. Chem.* **1996**, *17*, 520−552.
(42) Halgren, T. A. Merck Molecular Force Field. III. Molecular Geometries and Vibrational Frequencies for MMFF94. *J. Comput. Chem.* **1996**, *17*, 553−586.
(43) Halgren, T. A. Merck Molecular Force Field. IV. Conformational Energies and Geometries for MMFF94. *J. Comput. Chem.* **1996**, *17*, 587−615.
(44) Halgren, T. A.; Nachbar, R. Merck Molecular Force Field. V. Extension of MMFF94 Using Experimental Data, Additional Computational Data, and Empirical Rules *J. Comput. Chem.* **1996**, *17*, 616−641.
(45) Halgren, T. A. MMFF VI. MMFF94s Option for Energy Minimization Studies. *J. Comput. Chem.* **1999**, *20*, 720−729.
(46) Halgren, T. A. MMFF VII. Characterization of MMFF94, MMFF94s, and Other Widely Available Force Fields for Conformational Energies and for Intermolecular-Interaction Energies and Geometries. *J. Comput Chem.* **1999**, *20*, 730−748.

JM030852K